Preparation of organocobalt(iii) complexes via O₂ activation

Møller, Mads Sondrup; Kongsted, Jacob; McKenzie, Christine J.

Preparation of Organocobalt(III) Complexes via O$_2$ Activation

Mads S. Møller, Jacob Kongsted, Christine J. McKenzie*

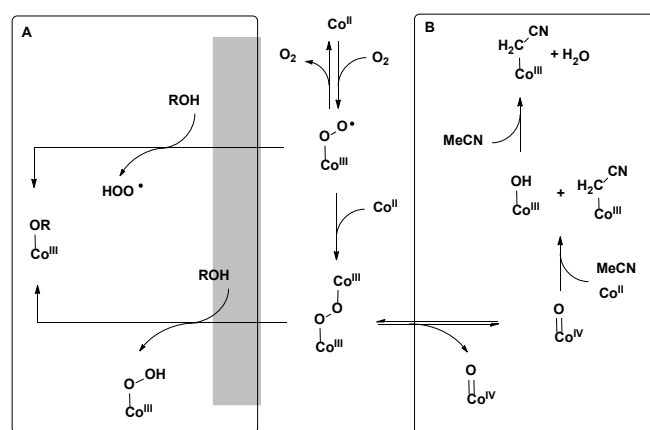The coupling of selective C–H activation with O$_2$ activation is an important goal for organic synthesis. New experimental and computational results, along with the results from experimental work accumulated over many decades, now unequivocally link O$_2$ activation with C–H activation by the classic Co(salen) complexes. A common holistic mechanistic framework can rationalise the formation of ostensibly diverse peroxo, superoxo, organo and alkoxide complexes of Co^{III}(salen). DFT calculations show that cobalt(III)superoxo, dicobalt(III)peroxo and cobalt(III)hydroperoxo complexes are all viable intermediates as participants in hydrogen atom transfer reactions, whereas a Co(IV)oxo intermediate is unlikely. The reaction conditions will determine the pathway followed and all pathways are initiated through the initial formation of a superoxo complex, Co^{III}(salen)(O$_2$•)(MeOH) (EPR: g = 2.025, A = 19 G). Organo and alkoxide ligands are derived from solvent media and the trends in reactivity reveal that combination of the pK_a and BDE of the C–H of the respective solvent substrates are important. These data explain why landmark, structurally characterized, μ_2-η^1, η^2-peroxide and η^1-superoxide Co(salen)–O$_2$ adducts were predominantly isolated from solvents with high C–H pK_a values (dmso, dmf, dma).

Introduction

Organocobalt complexes have been widely studied for at least six decades in the context of models for vitamin B$_{12}$. They are prepared by the reaction of Co(I) complexes with iodoalkanes, Co(III)halides with Grignard reagents,[1] and, more rarely, by the carbonylation of aliphatic alcohols with Co(II) and Co(III) precursors using CO.[2] Sporadic reports also document formation of organocobalt complexes without identifiable pathways.[3,4] For example, half a century ago Cesari *et al.*[5] described the crystal structures of Co^{III}(salen) (salen = N,N'-Bis(salicylidene)ethylenediamine) complexes containing C-coordinated cyanomethylene and acetonyl ligands which were derived from the solvents acetonitrile and acetone, respectively. In a subsequent patent they recognised that O$_2$ had been important for the preparations but no mechanism was suggested.[6] Around the same time Schaefer *et al.* reported the structural characterization of landmark biomimetic Co^{III}(salen)–O$_2$ adducts[7,8] that have served as important models for O$_2$ binding as either superoxido or peroxido ligands in heme and non-heme enzymes. In this work they also happened upon a Co^{III}(3F-salen)-acetonyl complex[9] (3F-salen = N,N'-Bis(3-flourosalicylidene)ethylenediamine) when attempting to prepare an oxygenated complex directly from Calvin's original sample of Co^{II}(3F-salen)(OH$_2$) prepared two decades earlier.[10] In parallel with this work, Nishinaga *et al.*[11] proposed that the formation of Co^{III}(salen) alkoxides (and hydroxides), which occurs in the presence of air in reactions of Co^{2+} and salen, includes a Hydrogen Atom Transfer (HAT) from the alcohol OH group to superoxide or peroxide complexes as depicted in Scheme 1A.

Department of Physics, Chemistry and Pharmacy, University of Southern Denmark, Campusvej 55, 5230 Odense M, Denmark. E-mail: mckenzie@sdu.dk.
† Footnotes relating to the title and/or authors should appear here.
Electronic Supplementary Information (ESI) available: [details of any supplementary information available should be included here]. See DOI: 10.1039/x0xx00000x

Scheme 1 The relationship between the mechanisms proposed by Nishinaga *et al.*[11] (A) and Nguyen *et al.*[12] (B) for the O$_2$ dependent formation of Co^{III}(OR) complexes of salen and the Co^{III}(CH$_2$CN) complex of ^{Br}HBA-Et. For simplicity overall charge is not depicted but it should be noted that the salen complexes in A are neutral and the complexes of ^{Br}HBA-Et in B are dianionic.

Recently Tilley and co-workers[12] proposed an O$_2$ activation pathway for the formation of organometallic cobalt(III) complexes of a planar tetranionic diamidodiphenol ligand, [Co^{III}(^{Br}HBA-Et)(CH$_2$CN)]$^{2-}$ (^{Br}HBA-Et = *N,N'*-(ethane-1,2-diyl)bis(5bromo-2-hydroxybenzamide) where the cyanomethylene ligand is derived from the acetonitrile solvent. This involves HAT from the MeCN C–H bond to a putative high-valent Co(IV)oxo complex derived from the homolytic Co–O–O–Co cleavage of an undetected μ-peroxido complex precursor. To rationalise the greater than 50% yields, a deprotonation of MeCN by an intermediate Co(III) hydroxide was invoked (Scheme 1B). It was suggested that this mechanism might be relevant also for the similar reactivity observed for the landmark Co(salen) complexes.

Scheme 1 illustrates the relationship between the aforementioned mechanistic proposals for HAT from substrate O–H or C–H bonds to Co(III)-superoxide, Co(III)$_2$-peroxide and Co(IV)-oxide intermediates as steps in the synthesis of Co(III)alkoxides/hydroxides/organo complexes via the O$_2$ activation by cobalt(II) complexes.

We have reinvestigated the preparation of organo, alkoxide and nitrito/nitro cobalt(III) complexes of the classic unsubstituted Co(salen) scaffold using a range of solvent substrates with C–H/O–H groups. On the basis the reaction conditions, the greater than 50% yields, spectroscopic evidence of a Co(III)superoxo intermediate and DFT calculations, we can now propose a common mechanistic framework for the formation of organo, $O_2^{\bullet-}$, O_2^{2-}, and alkoxide, complexes of Co(salen). This involves consecutive O_2 and C–H activations and can use Co(III)superoxide, Co(III)peroxide and Co(III)hydroperoxide intermediates in alternative pathways. We find no support for the participation of a Co(IV)oxo complex in the role of H atom acceptor.

Results and Discussion

Exposure of solutions of Co(salen) dissolved in nitromethane, trifluoroethanol, acetone/methanol, acetophenone/methanol and acetonitrile/methanol to air results in colour changes from reddish-orange to emerald green or brown and $Co(salen)(CH_2NO_2)$, $Co(salen)(OCH_2CF_3)$, $Co(salen)(CH_2COCH_3)$, $Co(salen)(CH_2COPh)$ and $Co(salen)(CH_2CN)$ are isolated respectively in yields between 50 – 70 %. Without MeOH as co-solvent in the reactions with acetone, acetophenone and acetonitrile, the organometallic complexes are not formed. Reactions are accelerated by bubbling pure oxygen (1 atm) through the mixtures. In air, a red alkoxide and a brown nitro complex of Co^{III}(salen) were isolated from reactions in 2,2,2-trifluroethanol and nitroethane respectively. The source of the nitrite in the latter, $Co(salen)(NO_2)$, which was isolated in a 40% yield, is at present unknown. There are two possibilities, (i) that the solvent was contaminated by nitrite or (ii) that the nitrite ligand is formed via an organometallic pathway akin to the pathway described below for the formation of the remaining complexes.

For simplicity in the following molecular-level discussions, it should be noted that the aforementioned formulae represent the core Co(salen)(L) formulation where the L is derived from the solvent substrate. In each case crystallography showed the Co(III) ion is hexacoordinate, binding either an axially coordinated O-coordinated methanol or water or by forming classic M(salen) dimers where interdimeric $Co\cdots O_{Ph\text{-}salen}$ bonds fill the axial position. For two of the compounds, $Co(salen)(CH_2COCH_3)$ and $Co(salen)(NO_2)$, both monomeric and dimeric phases were structurally characterized (Fig. 1 and SI Fig. S9-S10, ESI). Thermogravimetric analysis (TGA) of bulk $[Co(salen)(NO_2)]_2\cdot(EtNO_2)$ revealed the mass equivalent loss of one $EtNO_2$ per two $Co(salen)(NO_2)$ at 110 °C. Further heating to 230 °C resulted in a second mass loss corresponding to one NO_2 per Co(salen). TGA on bulk $Co(salen)NO_2(H_2O)$ showed the mass equivalent loss of one water molecule per Co(salen) at 122 °C (SI Fig. S1, ESI).

Crystal structures

$[Co(salen)(CH_2NO_2)]_2\cdot(2\ MeNO_2)$, $Co(salen)(CH_2COCH_3)(MeOH)$,[5] $Co(salen)(CH_2COCH_3)(H_2O)$, $[Co(salen)(CH_2COCH_3)]_2\cdot(C_6H_6)$, $[Co(salen)(CH_2COPh)]_2$ and $[Co(salen)(CH_2CN)]_2\cdot(C_6H_6)$, $[Co(salen)(OCH_2CF_3)]_2\cdot(4\ CF_3CH_2OH)$ and $Co(salen)(NO_2)$ are shown in Fig. 1. $Co(salen)(NO_2)$ occurs in two phases, one containing the dimer and the other a monomer, $[Co(salen)(NO_2)]_2\cdot(EtNO_2)$ and
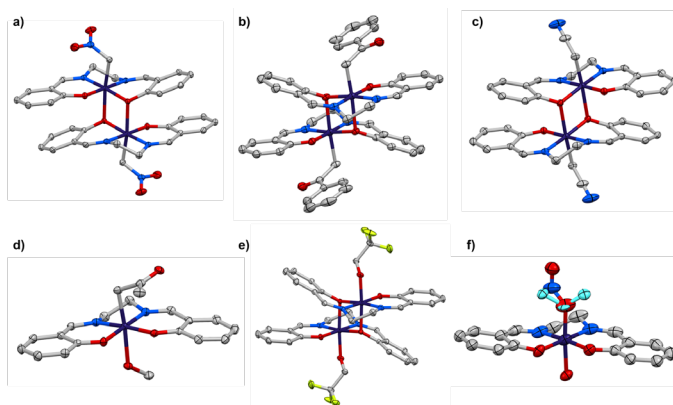

Fig. 1 Selected crystal structures. **(a)** $[Co(salen)(CH_2NO_2)]_2\cdot(2\ MeNO_2)$, **(b)** $[Co(salen)(CH_2COPh)]_2$, **(c)** $[Co(salen)(CH_2CN)]_2\cdot(C_6H_6)$, **(d)** $Co(salen)(CH_2COCH_3)(MeOH)$, **(e)** $[Co(salen)(OCH_2CF_3)]_2\cdot(4\ CF_3CH_2OH)$, **(f)** $Co(salen)(NO_2)(H_2O)$. The nitrite ligand in $Co(salen)(NO_2)(H_2O)$ is disordered between nitro and nitrito coordination, the minor component is coloured cyan. Thermal ellipsoids are drawn at 50 % probability for **a-e** and at 30 % probability for **f**, H atoms and non-coordinating solvate molecules are omitted for clarity.

$Co(salen)(NO_2)(H_2O)$, respectively. Another phase of $Co(salen)(CH_2CN)$ with a 1D coordination polymer structure is known.[5]

All the complexes show octahedral Co centres (Fig. 1), consistent with the +3 oxidation state and with angles deviating by an average of 0.03° from 90°. As expected, the salen ligand is almost planar in the monomeric complexes with the planes of the phenol rings twisted 8.15°, 6.44° and 5.21° from each other in $Co(salen)(CH_2COCH_3)(MeOH)$, $Co(salen)(CH_2COCH_3)(H_2O)$, $Co(salen)(NO_2)(H_2O)$ respectively. All Co–C bonds lie within the range of 1.97 Å to 2.00 Å, similar to those found earlier for related compounds.[13,14] The dimeric structures show two different Co–O_{phenol} bond lengths, the longer bond to the μ-O ranging from 1.924-1.938 Å in the extremes of $[Co(salen)(CH_2COCH_3)]_2\cdot(C_6H_6)$ and $[Co(salen)(NO_2)]_2\cdot(EtNO_2)$ and the shorter Co–O bond to the terminal phenolato oxygen atom (1.880-1.893 Å). Characteristically[15] the salen ligand deviates more from planarity in the dimeric complexes. The angles between the planes of the phenol rings range from 15.29-23.10°.

Spectroscopic characterisation

IR spectra show that the salient bands for the functional groups in the C-coordinated ligands are shifted towards lower wavenumbers compared to the parent organic molecules (Fig. 2, Table 1). Such a shift towards lower wavenumbers might be expected to be associated with an increase in bond length, but in this case the relevant bond lengths of the parent organic molecules are virtually identical to those of the coordinated species (Table 1).[16] Two bands at 1632 cm^{-1} and 1622 cm^{-1} in the IR spectrum of $Co(salen)(CH_2COPh)$ are due to aromatic C=C stretching and confirm the presence of an additional phenyl group. Accordingly (due to lack of phenyl group in axial co-ligand), only one C=C stretch appears in the spectra of the other complexes.

The crystal structures do not show any significant intra- or intermolecular interactions and the differences in the positions of the bands for the nitro, carbonyl and nitrile groups of the ligated *vs.*
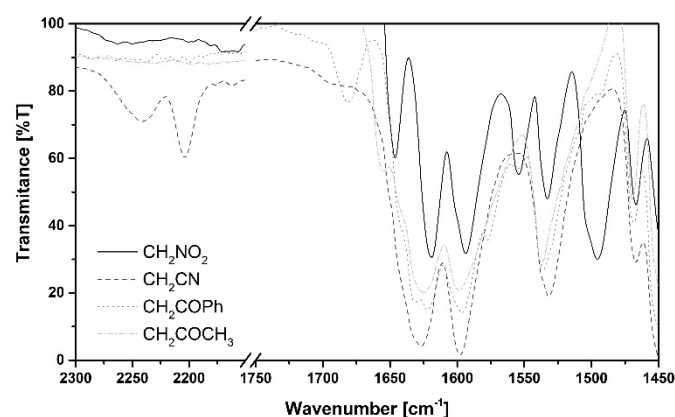
Fig. 2 ATR-FT IR spectra of [Co(salen)(CH$_2$NO$_2$)]$_2$·(MeNO$_2$), Co(salen)(CH$_2$COCH$_3$)(MeOH), [Co(salen)(CH$_2$COPh)]$_2$ and Co(salen)CH$_2$CN.

Table 1 Selected vibrational frequencies and bond lengths for the organocobalt and the solvent molecules from which they are derived.

Compound	Group	ν_{group} [cm^{-1}]	Bond length (group) [Å]
Co(salen)(CH$_2$NO$_2$)	NO$_2$	1496	1.229(7)
CH$_3$NO$_2$		1570[a]	1.21(2)[b]
Co(salen)(CH$_2$COCH$_3$)	C=O	1655	1.228(4)
(CH$_3$)$_2$CO		1720[a]	1.22(3)[b]
Co(salen)(CH$_2$COPh)		1681	1.229(2)
CH$_3$COPh		1702[a]	-
Co(salen)(CH$_2$CN)	C≡N	2204	1.151(3)
CH$_3$CN		2258[a]	1.157[b]

[a] IR stretches for solvents obtained from NIST[17]. [b] Bond lengths for solvents obtained from Sutton *et al.*[16]

free species are of such large magnitude that intermolecular interactions can be ruled out as being the main cause. The decrease in band position in the organometallic complexes is, therefore, most likely related to the inductive effect of the group being coordinated to Co(III).

In the ^{1}H NMR spectra, the signals for the protons of the coordinating methylene groups are shifted downfield compared with the corresponding methyl signals of the parent solvents. For instance, these appear at 2.88 ppm in the spectrum of Co(salen)(CH$_2$COCH$_3$) compared to 2.08 ppm for acetone (Fig. 3a). In contrast the distal acetyl methyl group signal is shifted upfield to 1.64 ppm. Reminiscent of the changes in the IR spectra, these field shifts could be due to the inductive effect of the highly charged Co(III) ion.[1,18] While the coordinated methylene group protons can be identified in ^{1}H NMR spectra, the carbon resonances of the coordinating methylene groups (C$_c$) are not apparent in the ^{13}C NMR spectra (*e.g.* Fig. 3b). The explanation for this is that the carbon is bonded directly to the quadrupole nucleus ^{59}Co (100% abundance, I = 7/2, Q = 0.42) and the T$_1$ relaxation is too fast to allow detection of the coupling. In addition, residual line broadening[19] means that in practice the signal for the coordinated carbon is undetectable. Although we cannot find this explicitly stated anywhere in the literature, presumably this is the reason that Co–C complexes have, to date, been characterised only by solution-state ^{1}H NMR spectroscopy.
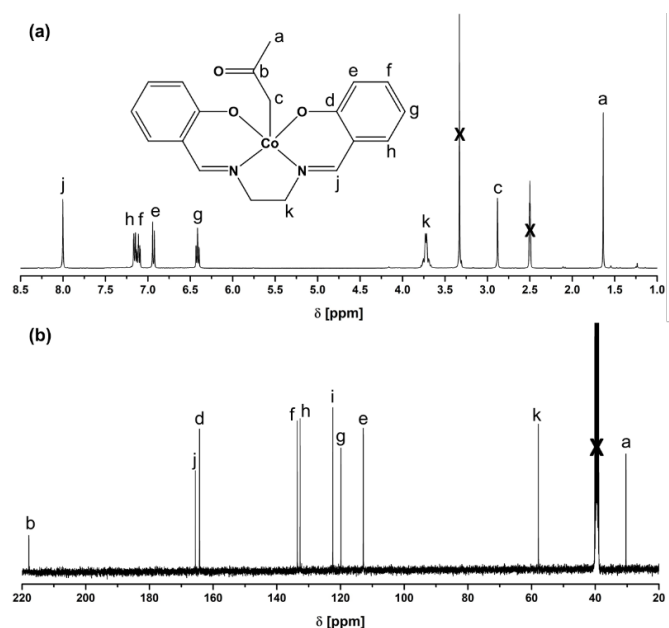

Fig. 3 (a) ^{1}H NMR spectrum (d$_6$-DMSO) and **(b)** ^{13}C NMR spectrum of Co(salen)(CH$_2$COCH$_3$)(MeOH) with assignments. Residual solvent peaks and H$_2$O are marked with X.

We turned, therefore, to solid-state ^{13}C CPMAS NMR spectroscopy and found that the coordinating methylene groups of the organocobalt complexes can be identified. The signals are however relatively broad due to poorly resolved coupling to the I = 7/2 Co nucleus (Fig. 4a,b). The signal at 19.1 ppm and the shoulder at 48.5 ppm are assigned to this group in the ^{13}C CPMAS NMR spectra of Co(salen)(CH$_2$COCH$_3$)(H$_2$O) and [Co(salen)(CH$_2$NO$_2$)]$_2$·(2 MeNO$_2$) respectively. Comparison of the integrals of these peaks with those of the ethylene backbone gives salen:CH$_2$C(O)CH$_3$ and salen:CH$_2$NO$_2$ ratios of 1:1, as expected. The resonances for the coordinating carbon atoms are shifted approximately 10 ppm upfield compared to the corresponding carbon atoms of the methyl groups in MeNO$_2$ and acetone (62.6 ppm and 30.6 ppm respectively), consistent with coordinated carbon being more shielded. Curiously, this can be contrasted to the downfield shifts observed for the protons attached to these coordinated methylene carbon atoms found in the solution state ^{1}H NMR spectra. These observations, in the complementary NMR and IR spectra, are consistent with the electrons in the C-coordinated ligand being delocalised towards the coordinating carbon atom and the cobalt atom. The resonances at 216.0 and 31.0 ppm in the spectrum of Co(salen)(CH$_2$COCH$_3$)(H$_2$O) are due to the carbonyl and methyl group of the coordinated acetonyl respectively. A resonance at 61.3 ppm in the spectrum of [Co(salen)(CH$_2$NO$_2$)]$_2$·(2 MeNO$_2$) is assigned to equimolar co-crystallised MeNO$_2$, consistent with TGA results (Fig. S1, ESI). The solid-state ^{13}C CPMAS NMR spectra also reveal the subtle environment differences that are lost on dissolution when compared with the solution-state spectra. To illustrate this, the spectrum of [Co(salen)(NO$_2$)]$_2$·(CH$_3$CH$_2$NO$_2$) (Fig. 4c) shows four resonances for the four crystallographically distinct imine carbons in the region 175 – 155 ppm and two signals for the phenoxy carbons as is consistent with the dimeric structure. By comparison there are only two imines (134.34, 133.94 ppm) in the solution state (Fig. S20, ESI). Resonances at 60.0 ppm and 56.0 ppm belong to the ethylene backbone in contrast to one at 58.02 ppm in
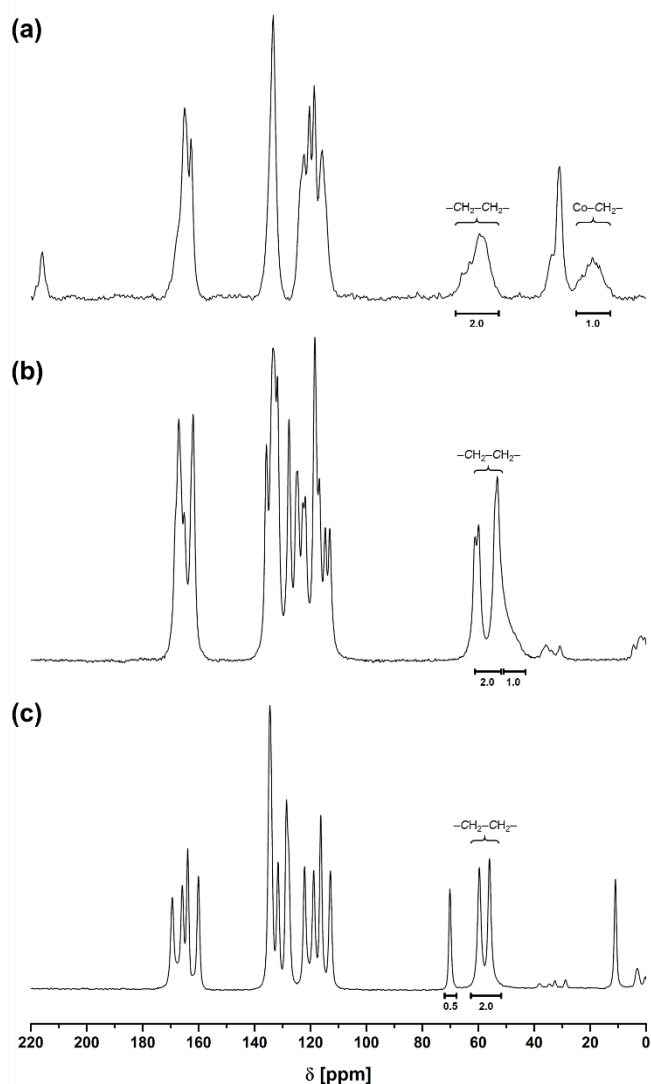
Fig. 4 ^{13}C CPMAS NMR spectrum of **(a)** [Co(salen)(CH$_2$COCH$_3$)(H$_2$O)] **(b)** [Co(salen)(CH$_2$NO$_2$)]$_2$·(MeNO$_2$) and **(c)** [Co(salen)NO$_2$]$_2$·(EtNO$_2$).

solution (Fig. S20, ESI).

The resonances at 70.1 ppm and 11.0 ppm are assigned to the co-crystallised EtNO$_2$ solvate and the integrals indicate a salen/EtNO$_2$ ratio of 2:1, entirely consistent with TGA measurements on [Co(salen)(NO$_2$)]$_2$·(CH$_3$CH$_2$NO$_2$) (Fig. S1, ESI).

Photolability

The homolytic cleavage of the Co–C bond in Co(salen)(CH$_2$COCH$_3$) to regenerate Co(salen) and an acetonyl radical is, not unexpectedly,[20] induced by light. Time-resolved UV-vis spectroscopy (Fig. 5) shows that the absorption bands, most noticeably those at 354 nm and 784 nm, disappear over a few minutes on irradiation (365 nm). A radical trapping experiment was carried out by exposing a d_6-DMSO solution of Co(salen)(CH$_2$COCH$_3$) (7.8 mM) and (2,2,6,6-tetramethylpiperidin-1-yl)oxyl (TEMPO) (62.4 mM) to light for 48 h at ambient temperature. A colour change from brownish green to red over this time indicated the formation of Co(salen) (Fig. S3, ESI). ^1H NMR spectra (Fig. 5) before and after irradiation

show that the characteristic signals around 3.9 ppm, corresponding to the ethylene backbone of Co(salen)(CH$_2$COCH$_3$) disappear, consistent with cleavage of the Co–C bond to produce the paramagnetic (NMR invisible) Co(II) species (Fig. 6). The acetonyl radical was trapped to form TEMPO–CH$_2$COCH$_3$, as evidenced by a signal at δ = 4.4 ppm corresponding to the methylene protons in the NMR spectrum. This shows also that acetone is generated and this might be occurring by H atom transfer to the acetonyl radical by PCET from a Co^{II}(salen) water complex. The ESI mass spectrum of the mixture shows Co(salen) and TEMPO–CH$_2$COCH$_3$ (Fig. S5).

Spectroscopic detection of superoxide intermediate

Time-resolved UV-visible spectroscopy shows that conversion of Co(salen) to Co(salen)(CH$_2$NO$_2$) in degassed nitromethane takes approximately 48 hours after exposure to air at ambient temperature. There is no sign of an intermediate in the time-resolved UV-vis spectra (Fig. S6). However, if the reaction is
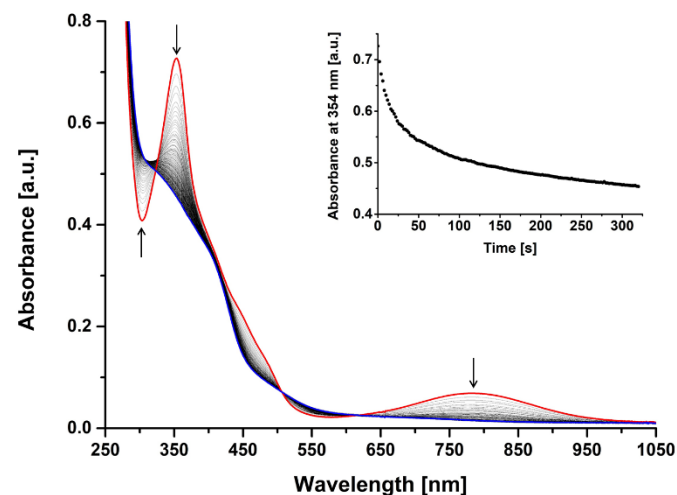
Fig. 5 Photoinduced homolytic cleavage of Co-C bond in Co(salen)(CH$_2$COCH$_3$) (0.1 mM, DCM) to afford Co(salen) and CH$_3$COCH$_2$• using a 365nm LED.
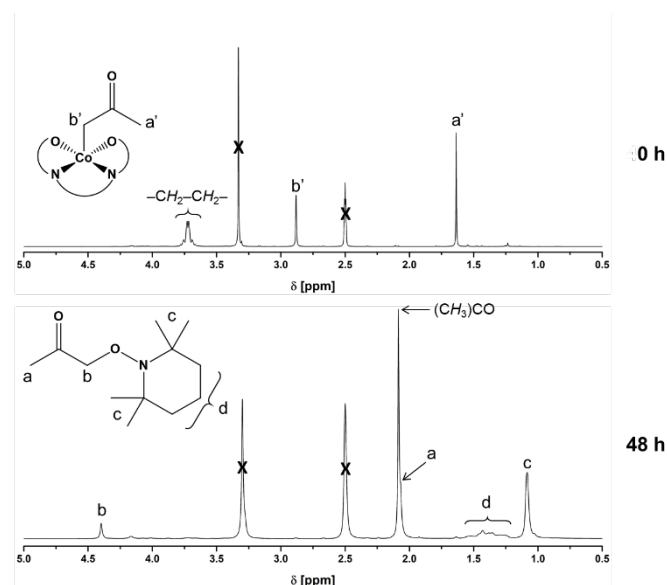

Fig. 6 ^1H NMR spectra (d_6-DMSO) of Co(salen)(CH$_2$COCH$_3$) and TEMPO before and after visible light irradiation at room temperature for 48 hours. Residual solvent peaks are marked with X.

carried out in acetone/methanol (3:2 V/V) while purging with O_2, after approximately 15 minutes an intermediate is detected using EPR spectroscopy (Fig. 7a). In turn, this signal disappears as the species is converted over the course of 45 minutes ($t_{1/2} \approx$ 22 min) to the carbon-coordinated product (Fig. 7b). The signal shows that the intermediate is a $S = 1/2$ species with hyperfine coupling to a ^{59}Co ($g = 2.025$, $A = 19$ G). This is assigned to the η^1-superoxo complex $Co(salen)(O_2^{\bullet})(MeOH)$. The g-value and hyperfine coupling constant are similar to those previously reported for this well-known class of compound.[21]

An axial MeOH ligand is included in the formulation because the C–H activation reaction of acetone, acetophenone or acetonitrile does not occur in the absence of MeOH as a co-solvent. Calculations of the g-value for the structures without,

or with, axial solvent ligands i.e., $Co(salen)(O_2^{\bullet})$ $Co(salen)(O_2^{\bullet})((CH_3)_2CO)$ and $Co(salen)(O_2^{\bullet})(MeOH)$, gave $g =$ 1.9675, 1.9593 and 1.9921, respectively, from which it is seen that the predicted g-value for $Co(salen)(O_2^{\bullet})(MeOH)$ is nearest the measured value. Even more importantly, mechanistic DFT calculations show that $Co(salen)(O_2^{\bullet})(MeOH)$ is the more stable of the three possibilities (see details below). These results concur with the formation of the Co(III)superoxo complex $Co(salen)(O_2^{\bullet})(MeOH)$, and the observations are furthermore entirely consistent with the proposal of a superoxo complex by Nishinaga *et al.*[22] as the crucial intermediate prior to the formation of cobalt(III)peroxyquinolato complexes when a Co(II) complex of a pentadentate diamine ligand related to salen was reacted with 2,6-di-*tert*-butylphenols in the presence of O_2.

Peroxo-bridged $Co^{III}(salen)$ complexes have been isolated from dmso, dmf, pyridine and dimethylacetamide (DMA).[23] These form by reactions of $Co^{II}(salen)$ with O_2 and along with the reactions described above, are depicted in Scheme 2. In benzene, DCM, acetone and DMA, EPR spectroscopy has shown that $Co^{II}(salen)$ possesses a $(d_{yz})^2(d_{zx})^2(d_{z^2})^2(d_{xy})^1(d_{x^2-y^2})^0$ electronic configuration,[24] thereby rationalising the inhibition of $Co^{II}(salen)$ oxygenation at room temperature in these particular solvents. By contrast the $(d_{yz})^2(d_{zx})^2(d_{xy})^2(d_{z^2})^1(d_{x^2-y^2})^0$ electronic configuration is present in coordinating solvents like pyridine, dmso and dmf.[24] MeOH has not been examined in this context *per se*, however, as a potentially coordinating solvent, and in the context of our observations that its presence is essential for the reactions where acetone, acetophenone and acetonitrile are the C–H substrates, it would seem likely that its axial coordination induces this electronic structure which is a pre-requisite for O_2 activation.

DFT calculations

Despite the wealth of experimental data available documenting the chemistry of Co(salen), this system has been scarcely addressed using DFT calculations.[25–27] Crucially the mechanism
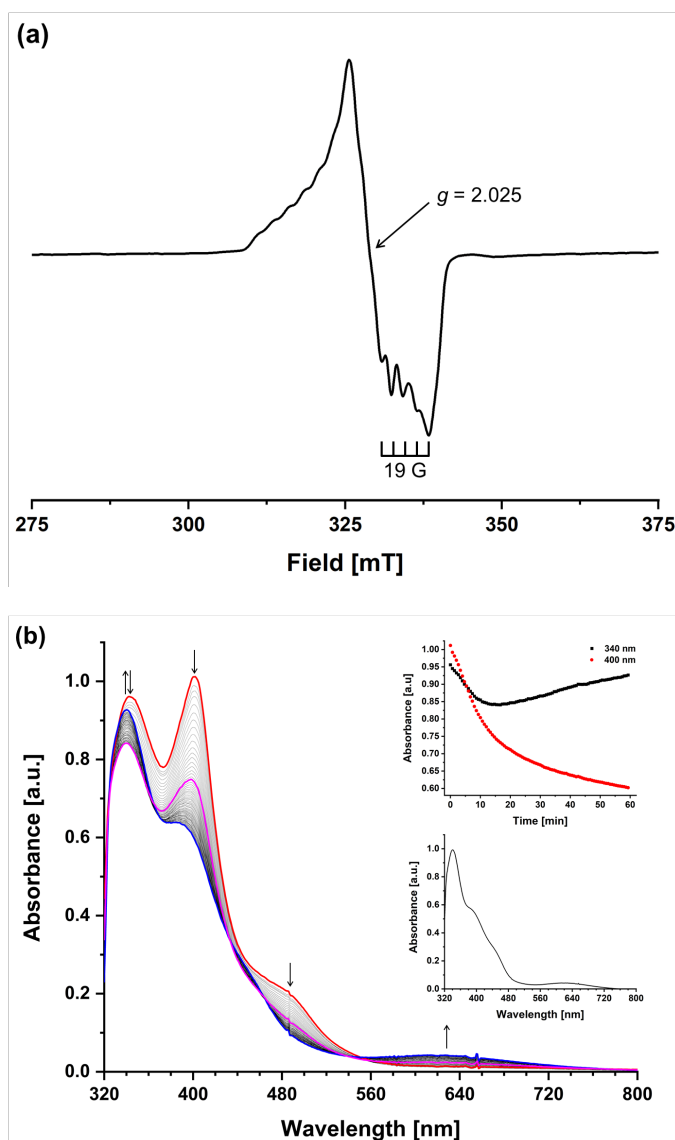

Fig. 7 (a) EPR spectrum of a solution of $Co(O_2)(salen)$ (acetone/methanol, 100 K, microwave frequency 9.30858 GHz). **(b)** Time-resolved conversion of Co(salen) (0.1 mM) to $Co(salen)(CH_2COCH_3)$ at 20 °C upon its reaction with O_2 in a degassed solution of acetone/methanol (3:2). Red trace is Co(salen), blue trace is t = 60 min, magenta trace is t = 15 min. Insert bottom: UV-vis spectrum of independently prepared $Co(salen)(CH_2COCH_3)$ in acetone/methanol (3:2).
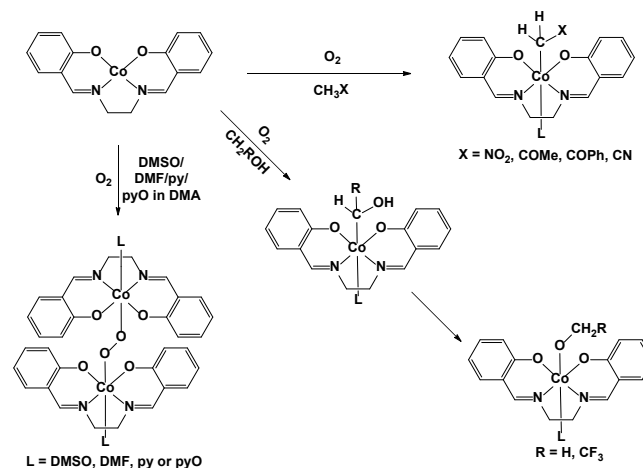
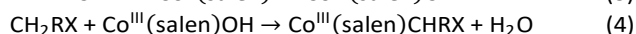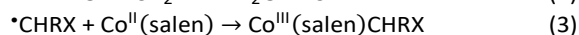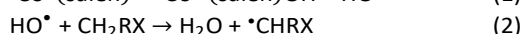**Scheme 2.** The products of reactions of Co(salen) when exposed to oxygen in different solvents. X = NO_2, $COCH_3$, COC_6H_5 and CN. L = DMSO, DMF, py, pyO.[23] L are the second axial ligands found in the crystal structures and important for the solution state O_2 activation. These are solvent-derived or a phenolato O atom from the other complex in a dimer.

of formation, and the reactivity of Co(salen)–O_2 adducts, have not been investigated. We have considered the routes to the organocobalt complexes, Co^{III}(salen)(CHRX) depicted in Scheme 3. The common starting point for all routes is the reaction of O_2 with Co^{II}(salen) (step i) to form the superoxide species Co^{III}(salen)($O_2^{\bullet}$)(MeOH) - the transient detected by EPR spectroscopy (Fig. 7a). Two alternative paths confront this species, reaction with the C–H of a substrate solvent molecule (step ii) or a second equivalent of Co^{II}(salen) (step v). In step ii, a hydrogen atom transfer (HAT) leads to the formation of a hydroperoxide complex Co^{III}(salen)OOH(MeOH), and the solvent-derived organic radical, $^{\bullet}$CHRX. From this point the final product, Co^{III}(salen)(CHRX)(MeOH), can be formed by either reaction of $^{\bullet}$CHRX with a second equivalent of Co^{II}(salen) (step iii) or the Co^{III}(salen)(OOH)(MeOH) can react with a second solvent molecule (step iv). The overall Co(salen):O_2 ratio would be 2:1.

An alternative route involves reaction of the initial, common Co^{III}(salen)($O_2^{\bullet}$)(MeOH) complex with a second equivalent of Co^{II}(salen) (step v) to give a peroxide-bridged complex $\{[(MeOH)(salen)Co^{III}]_2(\mu\text{-}O_2)\}$. There is structural precedence for such a complex (Scheme 2). Significantly, in the context of our results, DMSO, DMF, py or DMA with pyO were the solvents used in the preparations of these complexes.[23] Step vi shows the homolytic cleavage of the O–O bond in $\{[(MeOH)(salen)Co^{III}]_2(\mu\text{-}O_2)\}$ to produce two equivalents of Co^{IV}(salen)(O)(MeOH) analogously to the proposal illustrated in Scheme 1B. Such a high-valent Co(IV)oxo can be regarded as relatively inaccessible and therefore highly speculative. If it was generated, however, it might abstract a H atom from a C–H bond (step vii) and this would result in the formation of a solvent-derived organic radical, $^{\bullet}$CHRX and equimolar Co^{III}(salen)(OH)(MeOH). From here Co^{III}(salen)(CHRX)(MeOH) can be formed by either reaction of $^{\bullet}$CHRX with a second equivalent of Co^{II}(salen) (step viii) or Co^{III}(salen)(OH)(MeOH) can react with a second solvent molecule (step ix). The Co(salen):O_2 ratio that would be needed for this pathway is 4:1. As an alternative to the homolytic cleavage of $\{[(MeOH)(salen)Co^{III}]_2(\mu\text{-}O_2)\}$, this complex could also react directly with the solvent forming two equivalents of the final product Co^{III}(salen)(CHRX)(MeOH) (step x) and H_2O_2. In this case the Co(salen):O_2 ratio required would be 2:1.

Fig. 8 shows the relative energy profile of the mechanism in which the common starting Co^{III}(salen)($O_2^{\bullet}$)(MeOH) reacts with acetonitrile. Step i, the formation of Co^{III}(salen)($O_2^{\bullet}$)(MeOH), is exergonic. An axial MeOH ligand (not shown in Fig. 8) stabilises this superoxide complex: calculations show that Co^{III}(salen)($O_2^{\bullet}$) is 23.2 kcal mol^{-1} higher in energy compared to Co^{III}(salen)($O_2^{\bullet}$)(MeOH). An axial acetonitrile ligand (Co^{III}(salen)($O_2^{\bullet}$)(MeCN) results in a complex which is only 18.3 kcal mol^{-1} lower in energy compared to Co^{III}(salen)($O_2^{\bullet}$). Of the two possible spin states (S = 1/2 and S = 3/2) for Co(II) in Co^{II}(salen), that with the lowest energy is the low spin S = 1/2. The subsequent HAT (step ii) is endergonic by 27.9 kcal mol^{-1}, due to formation of an organic radical, resulting in a total energy

slightly higher than the starting energy. That this increase in energy is caused by formation of a radical, is verified by the subsequent exergonic step iii (-40.6 kcal mol^{-1}) in which complexation of the radical by a second molecule of Co^{II}(salen) leads to the organocobalt complexes that have been isolated. By designating formation of H_2O_2 as the other product in step iv this process is endergonic. An exergonic process with a more complicated mechanism and production of O_2 and water is also feasible. For this, the Co(salen):O_2 ratio needed will be 4:1 and the energy of the final stage will be -52.9 kcal mol^{-1} compared to -25.5 kcal mol^{-1}. We note that H_2O_2 can potentially participate in reactions which result in formation of additional Co^{III}(salen)(CHRX) (Eqs. 1-4):

$$H_2O_2 + Co^{II}(salen) \rightarrow Co^{III}(salen)OH + HO^{\bullet} \qquad (1)$$
$$HO^{\bullet} + CH_2RX \rightarrow H_2O + {}^{\bullet}CHRX \qquad (2)$$
$${}^{\bullet}CHRX + Co^{II}(salen) \rightarrow Co^{III}(salen)CHRX \qquad (3)$$
$$CH_2RX + Co^{III}(salen)OH \rightarrow Co^{III}(salen)CHRX + H_2O \qquad (4)$$

Full conversion of Co(salen) would be achieved by reaction of Co^{III}(salen)OH with the solvent (eq. 4). This is evidently possible for more acidic solvents like nitromethane and acetone.[28] This would also result in a Co(salen):O_2 ratio of 4:1 and matches the mechanistic proposals made by Schaefer et al.[9] who proposed that Co(III) superoxo or peroxo intermediates may attack the C-H bond of acetone.

The alternative pathway of Co^{III}(salen)($O_2^{\bullet}$)(MeOH) reacting with a second Co^{II}(salen) and formation of a peroxide-bridged complex $\{[(MeOH)(salen)Co^{III}]_2(\mu\text{-}O_2)\}$ step(v) is computed to be more favorable than reaction with solvent (step ii). However, an onwards conversion by homolytic O–O cleavage to two Co^{IV}(salen)(O)(MeOH) complexes presents a very large barrier of 40.1 kcal mol^{-1} (step vi); the most endergonic reaction considered according to the calculations. Of the three possible spin states (S = 1/2, S = 3/2 and S = 5/2) for Co(IV) in Co^{IV}(salen)(O)(MeOH), the S = 1/2 spin state is lowest in energy. Formation of Co^{IV}(salen)(O) by a mononuclear mechanism through homolytic cleavage of Co^{III}(salen)(OOH)(MeOH) is also not energetically accessible: An energy state 157.2 kcal mol^{-1} higher than the starting energy was obtained. By contrast, conversion of the $\{[(MeOH)(salen)Co^{III}]_2(\mu\text{-}O_2)\}$ to Co^{III}(salen)(CHRX)(MeOH) and H_2O_2 (step x) presents an energy barrier which is 22.4 kcal mol^{-1} smaller than that for the homolytic O–O cleavage (step vi). Experimental verification of this pathway by H_2O_2 detection is however not possible since Co^{II}(salen) will immediately catalyse H_2O_2 disproportionation.

Despite being thermodynamically accessible according to the DFT calculations, $\{[(MeOH)(salen)Co^{III}]_2(\mu\text{-}O_2)\}$ could not be isolated from the reaction mixture. This suggests that kinetics plays a vital role in the outcome of the reaction. Step v can be viewed as an oxygen concentration dependent equilibrium, thus Co^{III}(salen)($O_2^{\bullet}$)(MeOH) will be favoured at high oxygen concentrations, while $\{[(MeOH)(salen)Co^{III}]_2(\mu\text{-}O_2)\}$ favoured at low oxygen concentrations. Based on the mol fraction of oxygen available in the solvents used,[29] Co(salen):O_2 ratios of
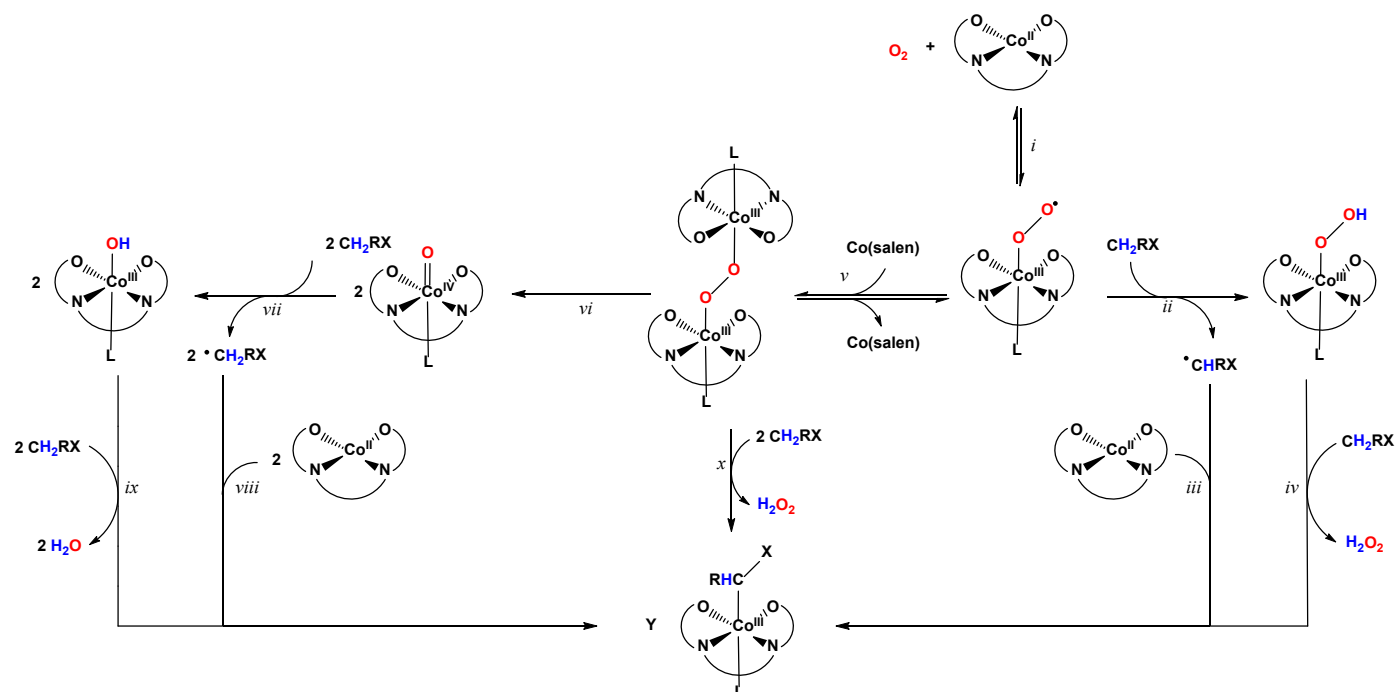
Scheme 3. Alternative proposals for the mechanism of formation of organo Co(salen) complexes. Y is the number of product complexes relative to Co(salen); Y = 2 when following the left and middle path and Y = 4 when following the right. L = MeOH, MeNO₂ or EtNO₂. X = CN, COCH₃, COPh or NO₂ and R = H or CH₃.
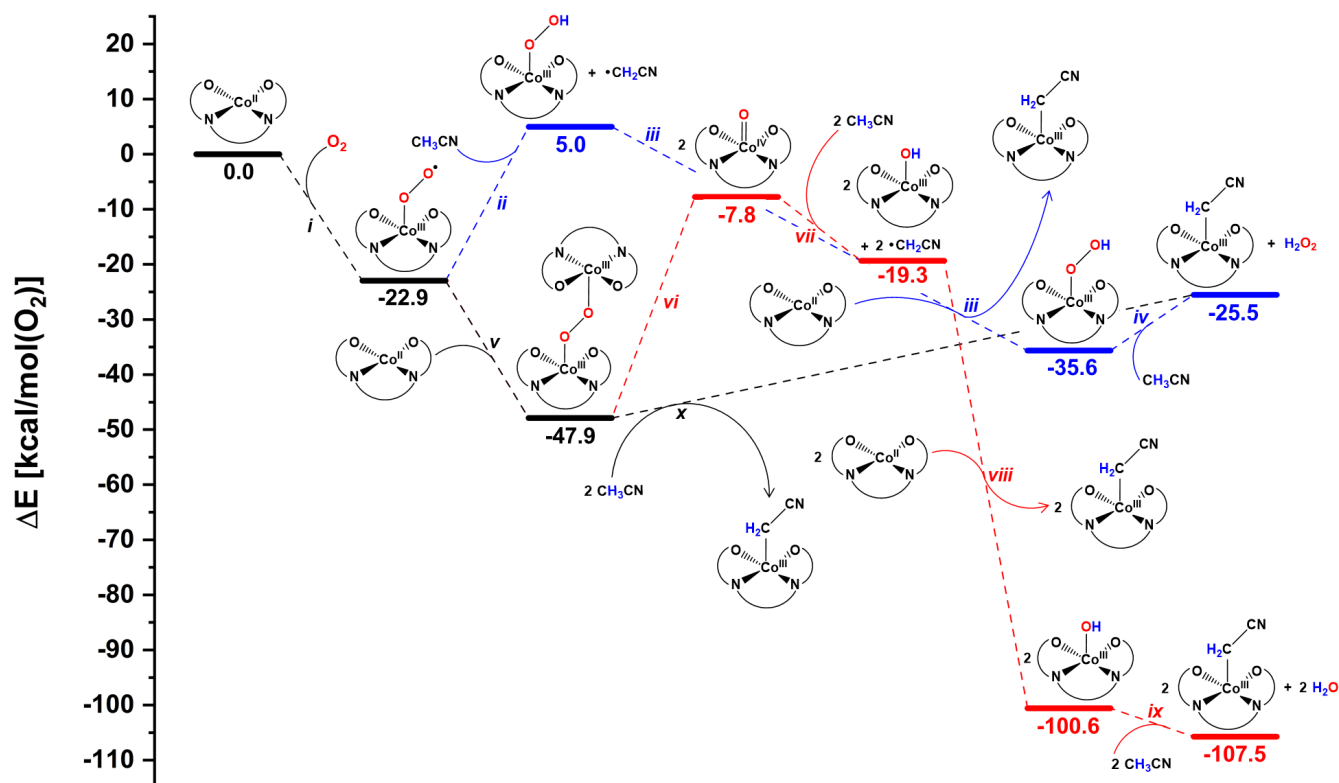

Fig. 8 Relative energy profile of the reaction mechanism in Figure 7. The axial MeOH ligand, present on all complexes in the calculations with exception of Co^{II}(salen), is omitted for clarity. Note that the axis shows the energy difference per O₂ molecule. An acetonitrile solvent model was used for the calculations. Co^{II}(salen), Co^{III}(salen)O₂ and Co^{IV}(salen)O are all $S = 1/2$

between 1.5-2.5:1 can be expected at room temperature in air at ambient pressure. Solvent-reagent molecules will be available in up to 600-fold excess compared to Co(salen). Given that $Co^{III}(salen)(O_2^\bullet)(MeOH)$ is likely to react with the first substrate it encounters, it is clearly far more likely to be a solvent molecule than a Co(salen). Reaction between $Co^{III}(salen)O_2^\bullet(MeOH)$ and the solvent substrate will be essentially pseudo first order.

Even though the formation of $\{[(MeOH)(salen)Co^{III}]_2(\mu\text{-}O_2)\}$ is not kinetically favourable, and its homolytic CoO–OCo cleavage product, $Co^{IV}(salen)(O)(MeOH)$, not favourable according to the calculations, for completeness we pursued computationally modelling the onward reaction of $Co^{IV}(salen)(O)(MeOH)$. While a HAT from substrate to a hypothetical $Co^{IV}(salen)(O)(MeOH)$ complex to give a $Co^{III}(salen)(OH)(MeOH)$ (step vii) is exergonic, again predominantly due to the neutralisation of $^\bullet CH_2CN$ by reaction with excess $Co^{II}(salen)$ (step viii), the product $Co^{III}(salen)(OH)(MeOH)$ must then subsequently act as a base to deprotonate the incoming substituting MeCN (step ix, Scheme 3). In order to address the feasibility of this reaction, the pK_a of its conjugate acid, $[Co^{III}(salen)(OH_2)(MeOH)]^+$, was determined by calculation. This gave 3.32 in DMSO (8.50 in H_2O). The pK_a value of MeCN in DMSO is 31.3.[30] These data imply that the equilibrium constant for step ix can be estimated to $K \approx 10^{-28}$. Thus, despite the fact that calculations indicate step ix is exergonic by 6.9 kcal mol^{-1}, the very low predicted equilibrium constant suggests that it is not feasible for $Co^{III}(salen)(OH)(MeOH)$ to act as a base for deprotonating the C–H bond of MeCN. In fact, this is consistent with experimental observations: $Co^{III}(salen)OH$ stirred in MeCN at 10 °C for 48 hours does not result in reaction. If this solution is heated to 70 °C a reduction of the complex to $Co^{II}(salen)$ occurs.[31]

To our knowledge only one transient Co(IV)oxo complex, $[(13\text{-}TMC)Co^{IV}(O)]^{2+}$, has been spectroscopically characterized.[32] Interestingly, and in stark contrast to the reactions described here, this was characterized in solutions containing acetone, yet formation of an acetonyl complex was not observed. HAT from C–H substrates with considerably lower BDEs of 73.7 kcal mol^{-1} to 80.3 kcal mol^{-1} were however achieved. The apparent differences in reactivity between $[(13\text{-}TMC)Co^{IV}(O)]^{2+}$ and the O_2-activated Co(salen) is striking, pointing to different metal-based intermediates and therefore mechanisms for C-H oxidation.

Table 2 lists the bond dissociation energies (BDE), pK_a values and electron-pair donor ability (D_s) where available for the solvents used in this study. With C–H BDEs in the range 96.3 – 99.3 kcal mol^{-1} and pK_a values ranging from 17.2 to 31.3, the solvents, in which the organometallic complexes form, are the least acidic of those that have been used in this and previous work. Notably, the D_s values are the largest for DMSO and DMF, solvents from which peroxide-bridged complexes have been isolated. The dependence on pK_a of the solvent suggest that the superoxide complex activates C–H bonds in the solvent molecule, and that this reaction has proton-transfer character.

Table 2 Bond dissociation energies (BDE), pK_a and electron-pair donor ability (D_s) for a selection of solvents.

Solvent	Bond	BDE [kcal mol^{-1}]	pK_a^a	D_s	Ref
Nitromethane	CH_3NO_2	99.3	17.2	9.0	30,33,34
Nitroethane	$CH_3CH_2NO_2$	98.1	16.7	-	30,33
Acetone	CH_3COCH_3	96.0	26.5	15.0	33–35
Acetophenone	$PhCOCH_3$	96.3	24.7	-	33,35
Acetonitrile	CH_3CN	97.0	31.3	12.0	30,33,34
DMSO	$CH_3S(O)CH_3$	94.0	35.1	27.5	30,33,34
DMF	$HCON(CH_3)_2$	105.0	-	24.0	34,36
Methanol	CH_3OH	96.1	-	18.0	33,34
	CH_3OH	105.2	29.0	18.0	33,34,37
TFE	CF_3CH_2OH	-	-	-	-
	CF_3CH_2OH	107.0	23.5	-	33,38
Water	H_2O	118.8	31.4	17.0	33,34,37

^{a} measured in DMSO, - not available

In addition to consideration of the solvent properties in terms of its function as a substrate, its ability to activate Co(salen) towards oxygenation through axial coordination is also important. This can be expected to be influenced by sterics. Indeed, this is borne out through a comparison of the reactivity of Co(salen) towards O_2 in DMF *vs.* DMA. These two solvents have the same D_s value,[34] however, oxygenation (to produce a peroxide-bridged dimer) occurs only in DMF.[24] It is however possible the trap the peroxide-bridged complex in DMA if an axial donor ligand, whose π-acceptor properties are non-existent or very small, is added.[23] This is consistent with our observation that MeOH is needed in order to ultimately achieve formation of the organo Co^{III}(salen) complexes derived from acetonitrile, acetone and acetophenone.

The proposal in Scheme 1A[11] makes the assumption that it is the O-H bond in alcohols that is attacked by the Co(III)superoxo or peroxo species. This does not seem thermodynamically likely because the C–H bond next to the alcohol group has a significantly lower BDE compared with the O–H bond (Table 2). In light of our observations we posit that the mechanism for the formation of Co(salen) alkoxides from MeOH and 2,2,2-triflouroethanol,[5,11] involves similar initial steps to the formation of the organometallic complexes. Thus, direct O_2 activation, gives a superoxide intermediate followed by HAT from the alcohol C–H group. The product, Co(salen)(CHROH) (R=H, CF_3) is however not stable because of the α-hydroxyl group and this allows for facile rearrangement to the isolated Co(salen)(OCH_2R) complexes (Fig. 9a). DFT calculations (Fig. 9b) support the proposal that H atom removal from the methylene C–H bond, rather than the alcohol O–H, is more favorable by 10.1 kcal mol^{-1} and that O coordination in the final product is more favorable than C coordination by a 4.2 kcal mol^{-1}. It can be noted that the alkoxy complexes of Co(III)salen are sensitive to water and quantitively converted to the corresponding hydroxy complexes when exposed to it. This contrasts to the organometallic complexes which are not hydrolysed.
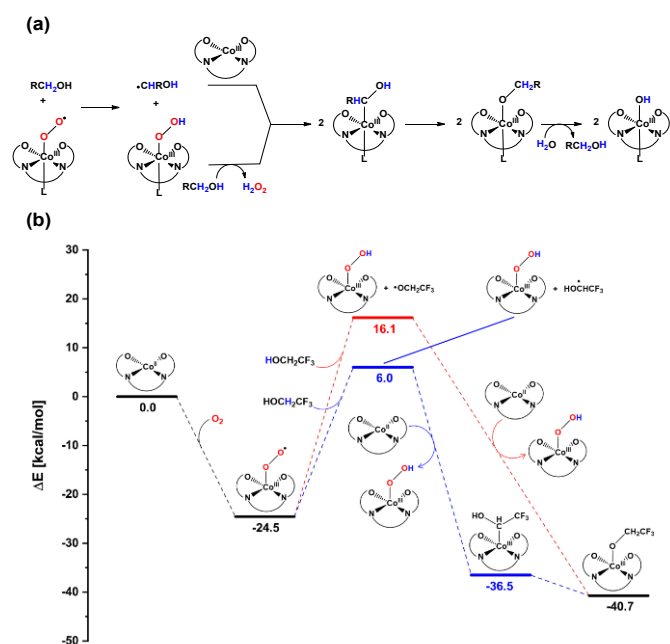
(a)

(b)

Fig. 9 (a) Proposed mechanism for formation of Co(salen) alkoxides, L = RCH$_2$OH. **(b)** Relative energy profile for the reaction between Co(salen) and CF$_3$CH$_2$OH. The axial CF$_3$CH$_2$OH ligand, present on all complexes in the calculations with exception of Co^{II}(salen), is omitted for clarity.

Conclusions

Co(III)salen superoxo and peroxo complexes have benchmarked the ways in which O$_2$ can bind to transition metal ions the superoxo complexes have been shown to oxidize C–H bonds of co-ligands,[39] and external organic substrates[22,40,41]. We show also that the pK_a value of the C–H bond of the terminal methyl groups the solvent media is critical for whether or not an O$_2$ adduct is stable, or whether it reacts further to give an organometallic complex. In turn, the stability of the organometallic product can be compromised by the group α to the coordinated carbon. We have presented a unifying mechanistic link between the formation of diverse, and in some cases, landmark peroxo, superoxo, organocobalt and alkoxide complexes of Co^{III}(salen).

A central question has been the identity of intermediate cobalt-based oxidant(s) for C–H oxidation formed by the activation of O$_2$ by Co(salen). Is this a Co(III)-superoxide, a dimeric Co(III)$_2$-μ-peroxide or a Co(IV)oxo intermediate? Our results point to the Co(III)-superoxide species at that which attacks C-H bonds under kinetic control. Thus, the initial stages are similar to pathway A in Scheme 1 - however it is C–H bonds of solvents, including alcohols (*i.e.* not their O–H bonds) that are susceptible to attack. The Co(III)$_2$-μ-peroxide is relatively stable, if formed, but may also be able to activate C–H bonds under appropriate conditions. We find no support for the involvement of a Co(IV)oxo species. In this context we note also that HAT from acetonitrile has not been observed for high-valent Fe(IV)oxo complexes where this solvent is used as the media for their formation.[42–45]

Author Contributions

M.S.M synthesized the compounds, performed the measurements, processed and analyzed the experimental and computational data, prepared the original draft and designed the figures. J.K. supervised the computational work. C.J.M conceived and supervised the work, managed resources and acquired funding. M.S.M and C.J.M. wrote the manuscript in consultation with J.K.

Conflicts of interest

There are no conflicts to declare.

Acknowledgements

Supporting Information

CCDC 2045576-2045584 contain the supplementary crystallographic data for this paper. These data can be obtained free of charge from The Cambridge Crystallographic Data Centre *via* www.ccdc.cam.ac.uk/data_request/cif. Additional information (synthesis, crystallography, photolytic experiment, computational methods, IR, NMR, TGA) can be found in link.

Notes and references

1   C. Floriani, M. Puppis and F. Calderazzo, *J Organomet Chem*, 1968, **12**, 209–223.
2   D. R. Chambers, R. E. Sullivan and D. B. C. Martin, *Organometallics*, 2017, **36**, 1630–1639.
3   N. A. Bailey, B. M. Higson and E. D. McKenzie, *Inorganic and Nuclear Chemistry Letters*, 1971, **7**, 591–593.
4   Y. Fujii and T. Yoshizawa, *Chem. Lett.*, 1976, **5**, 117–120.
5   M. Cesari, C. Neri, G. Perego, E. Perrotti and A. Zazzetta, *J. Chem. Soc. D*, 1970, **0**, 276–277.
6   C. Neri, E. Perrotti, US3787464A, 1974.
7   R. S. Gall, J. F. Rogers, W. P. Schaefer and G. G. Christoph, *J. Am. Chem. Soc.*, 1976, **98**, 5135–5144.
8   W. P. Schaefer, B. T. Huie, M. G. Kurilla and S. E. Ealick, *Inorg. Chem.*, 1980, **19**, 340–344.
9   W. P. Schaefer, R. Waltzman and B. T. Huie, *J. Am. Chem. Soc.*, 1978, **100**, 5063–5067.
10 R. H. Bailes and M. Calvin, *J. Am. Chem. Soc.*, 1947, **69**, 1886–1893.
11 A. Nishinaga, T. Kondo and T. Matsuura, *Chem. Lett.*, 1985, **14**, 905–908.
12 A. I. Nguyen, R. G. Hadt, E. I. Solomon and T. D. Tilley, *Chem. Sci.*, 2014, **5**, 2874–2878.

13 K. L. Brown, S. Cheng, X. Zou, J. Li, G. Chen, E. J. Valente, J. D. Zubkowski and H. M. Marques, *Biochemistry*, 1998, **37**, 9704–9715.

14 T. G. Pagano, L. G. Marzilli, M. M. Flocco, C. Tsai, H. L. Carrell and J. P. Glusker, *J. Am. Chem. Soc.*, 1991, **113**, 531–542.

15 S. Brückner, M. Calligaris, G. Nardin and L. Randaccio, *Acta Crystallogr. B Struct. Crystallogr. Cryst. Chem.*, 1969, **25**, 1671–1674.

16 L. E. Sutton and H. J. M. Bowen, *Tables of Interatomic Distances and Configuration in Molecules and Ions*, 1958.

17 NIST Chemistry WebBook, https://webbook.nist.gov/chemistry/, (accessed May 26, 2019).

18 G. Costa, G. Mestroni, G. Tauzher and L. Stefani, *J Organomet Chem*, 1966, **6**, 181–187.

19 D. Doddrell and A. Allerhand, *Proc. Natl. Acad. Sci. USA*, 1971, **68**, 1083–1088.

20 V. Balzani, L. Moggl, F. Scandola and V. Carassiti, *Inorganica Chimica Acta Reviews*, 1967, **1**, 7–34.

21 B. M. Hoffman, D. L. Diemente and F. Basolo, *J. Am. Chem. Soc.*, 1970, **92**, 61–65.

22 A. Nishinaga, H. Tomita, K. Nishizawa, T. Matsuura, S. Ooi and K. Hirotsu, *J. Chem. Soc., Dalton Trans.*, 1981, 1504.

23 C. Floriani and F. Calderazzo, *J. Chem. Soc., A*, 1969, 946.

24 E. Ochiai, *J. Chem. Soc., Chem. Commun.*, 1972, 489–490.

25 N. J. Henson, P. J. Hay and A. Redondo, *Inorg. Chem.*, 1999, **38**, 1618–1626.

26 A. Kochem, H. Kanso, B. Baptiste, H. Arora, C. Philouze, O. Jarjayes, H. Vezin, D. Luneau, M. Orio and F. Thomas, *Inorg. Chem.*, 2012, **51**, 10557–10571.

27 A. G. Starikov, V. I. Minkin and A. A. Starikova, *Struct. Chem.*, 2014, **25**, 1865–1871.

28 A. Bigotto, G. Costa, G. Mestroni, G. Pellizer, A. Puxeddu, E. Reisenhofer, L. Stefani and G. Tauzher, *Inorganica Chimica Acta Reviews*, 1970, **4**, 41–49.

29 R. Battino, Ed., *Oxygen and Ozone: Solubility Data Series (Volume 7)*, Pergamon, 1981.

30 W. S. Matthews, J. E. Bares, J. E. Bartmess, F. G. Bordwell, F. J. Cornforth, G. E. Drucker, Z. Margolin, R. J. McCallum, G. J. McCollum and N. R. Vanier, *J. Am. Chem. Soc.*, 1975, **97**, 7006–7014.

31 K. Aoki, S. Minami, US4746748A, 1988.

32 B. Wang, Y.-M. Lee, W.-Y. Tcho, S. Tussupbayev, S.-T. Kim, Y. Kim, M. S. Seo, K.-B. Cho, Y. Dede, B. C. Keegan, T. Ogura, S. H. Kim, T. Ohta, M.-H. Baik, K. Ray, J. Shearer and W. Nam, *Nat. Commun.*, 2017, **8**, 14839.

33 Y.-R. Lou, *Comprehensive Handbook of Chemical Bond Energies*, CRC Press, 2007.

34 M. Sandström, I. Persson, P. Persson, E. K. Euranto, T. Brekke, D. W. Aksnes and T. Tokii, *Acta Chem. Scand.*, 1990, **44**, 653–675.

35 F. G. Bordwell and J. A. Harrelson Jr, *Can J Chem*, 1990, **68**, 1714–1718.

36 Y.-R. Luo, *Comprehensive handbook of chemical bond energies*, CRC Press, 2007.

37 W. N. Olmstead, Z. Margolin and F. G. Bordwell, *J. Org. Chem.*, 1980, **45**, 3295–3299.

38 L. M. Huffman, A. Casitas, M. Font, M. Canta, M. Costas, X. Ribas and S. S. Stahl, *Chem. Eur. J*, 2011, **17**, 10643–10650.

39 M. S. Vad, A. Nielsen, A. Lennartson, A. D. Bond, J. E. McGrady and C. J. McKenzie, *Dalton Trans.*, 2011, **40**, 10698–10707.

40 A. Nishinaga, H. Tomita, M. Oda and T. Matsuura, *Tetrahedron Lett.*, 1982, **23**, 339–342.

41 T. Corona, S. K. Padamati, F. Acuña-Parés, C. Duboc, W. R. Browne and A. Company, *Chem. Commun.*, 2017, **53**, 11782–11785.

42 R. Singh, G. Ganguly, S. O. Malinkin, S. Demeshko, F. Meyer, E. Nordlander and T. K. Paine, *Inorg. Chem.*, 2019, **58**, 1862–1876.

43 J. P. Bigi, W. H. Harman, B. Lassalle-Kaiser, D. M. Robles, T. A. Stich, J. Yano, R. D. Britt and C. J. Chang, *J. Am. Chem. Soc.*, 2012, **134**, 1536–1542.

44 C. Wegeberg, W. R. Browne and C. J. McKenzie, *ACS Catal.*, 2018, **8**, 9980–9991.

45 J.-U. Rohde, J.-H. In, M. H. Lim, W. W. Brennessel, M. R. Bukowski, A. Stubna, E. Münck, W. Nam and L. Que, *Science*, 2003, **299**, 1037–1039.

TOC
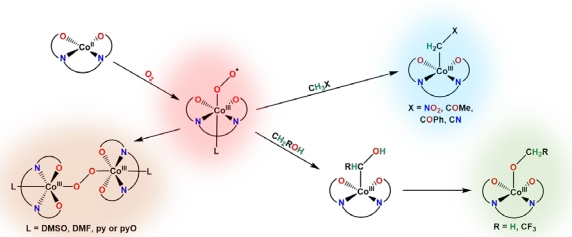
ORCID IDs

Mads Sondrup Møller 0000-0003-1674-7742

Jacob Kongsted 0000-0002-7725-2164

Christine J. McKenzie 0000-0001-5587-0626